J. Fluid Mech. (2026), *vol.* 1045, R1, doi:10.1017/jfm.2026.12145



Capillary–gravity-wave resistance of a translating, pulsating line source

Haim Diamant[1] **and Elie Raphaël**[2]

[1]School of Chemistry and Center for Physics and Chemistry of Living Systems, Tel Aviv University, 69978 Tel Aviv, Israel

[2]UMR CNRS Gulliver 7083, ESPCI Paris, PSL Research University, 75005 Paris, France

Corresponding authors: Haim Diamant, hdiamant@tau.ac.il; Elie Raphaël, elie.raphael@espci.fr

(Received 17 July 2026 UTC; revised 21 August 2026 UTC; accepted 4 September 2026 UTC)

A pressure disturbance in steady rectilinear translation applied at a capillary–gravity interface radiates waves only above a minimum speed c_{min}, where it experiences a wave resistance; below this threshold it generates no waves, and the response is merely a localised deformation of the interface around the source, free of wave resistance. Modulating the source amplitude at a frequency Ω shifts the forcing to the sideband pair $kV \pm \Omega$, where k is the wavenumber and V is the translation speed, opening resonance conditions absent from the steady problem; radiation then sets in below the steady threshold c_{min}. Here, we derive the mean wave resistance $\langle R \rangle$ of a line source in closed form, and show it to be strictly positive at every non-zero speed V: the drag-free below-threshold regime disappears for any $\Omega \neq 0$. Crossing the radiation transitions – where the group velocity matches the source speed – produces integrable resonant peaks in $\langle R \rangle$, whose exponents we derive, including at the cusp where two transition branches merge. Below threshold, where a steadily moving source feels no drag, $\langle R \rangle$ rises from zero as $V\Omega^5$. Throughout, surface tension is essential to $\langle R \rangle$: because it controls the short, dominant capillary-scale waves, discarding it misrepresents $\langle R \rangle$ over almost the entire speed–frequency plane.

Key words: capillary waves, surface gravity waves, wave-structure interactions

1. Introduction

A disturbance moving along a fluid interface can radiate waves and, in doing so, experience a resistive force, the wave resistance. This concept was developed by Havelock (1918) for gravity waves on deep water, in the wake of the classical studies of ship waves by Kelvin (1887) and the towing experiments of Froude (1874). This Rapid article concerns a line

© The Author(s), 2026. Published by Cambridge University Press.

https://doi.org/10.1017/jfm.2026.12145 Published online by Cambridge University Press

disturbance on a capillary–gravity interface of an inviscid fluid. For a source translating steadily at constant speed V in this geometry, the wave resistance has been calculated explicitly by Raphael & de Gennes (1996) (hereafter RdG)

$$R = \begin{cases} \dfrac{p^2}{\gamma}\left[1-(c_{min}/V)^4\right]^{-1/2}, & V > c_{min}, \\ 0, & 0 \le V < c_{min}, \end{cases} \tag{1.1}$$

where p is the force per unit length exerted by the localised pressure source, so that R is itself a force per unit length, and $c_{min} = (4g\gamma/\rho)^{1/4}$ is the minimum phase speed, set by the gravity g, surface tension γ and density ρ of the liquid. Below c_{min} the source radiates no waves, and the response is a deformation of the interface localised around the source.

Many interfacial sources of practical interest are, however, not steady (Dode *et al.* 2022; Arutkin *et al.* 2026). A floating body that bobs while advancing, or a vertically vibrating probe scanning the surface, imposes a pressure field whose amplitude is modulated at some frequency Ω. A source that translates uniformly while pulsating is a classical problem of dispersive wave radiation (Lighthill 1967); for pure-gravity waves a resonance occurs at $\Omega V/g = 1/4$ (Kaplan 1957; Dagan & Miloh 1982), and in the gravity-free limit its capillary counterpart is a critical resonance at $\Omega\gamma/(\rho V^3) = 4/27$ (§ 6). When both act together, by contrast, the phase speed has a minimum, c_{min}, which sets the below-threshold regime of (1.1), where $R = 0$ for a source translating steadily. The radiated wave field of the corresponding pulsating problem was obtained by Pramanik (1980), who partitioned the speed–frequency quadrant into regions of different wave content but did not address the wave resistance, which is our subject here. Unsteady motion is known to lift the below-threshold suppression: an accelerated source – one that changes speed or direction – radiates at $V < c_{min}$ (Chepelianskii *et al.* 2008; Closa *et al.* 2010), as does a laterally oscillating one. Roccuzzo & Herault (2026) recently modelled the wake of a slaloming swimmer as a superposition of uniformly translating pulsating sources, computing the mean wave drag numerically and finding secondary peaks below and above c_{min}. Their elementary source is the same object as ours, but differently forced: a fixed amplitude with oscillating transverse position spreads the excitation over harmonics of the slalom frequency weighted by Bessel factors, whereas amplitude modulation here gives the single sideband pair $kV \pm \Omega$, where k is the wavenumber. Our subject is the wave resistance of that elementary source itself, in closed form.

In this Rapid article we compute the wave resistance of this line source exactly. An amplitude modulation displaces the forcing to the sidebands $kV \pm \Omega$, opening resonance conditions absent from the steady problem (Pramanik 1980). We obtain the cycle-averaged wave resistance $\langle R\rangle$ in closed form, by contour integration, as a finite sum over the radiating modes, and show it to be strictly positive at every speed $V > 0$ once $\Omega \neq 0$. Across the radiation transitions it develops integrable resonant singularities whose exponents we derive, including at the cusp where two saddle-node branches merge; the steady RdG result is recovered continuously as $\Omega \to 0$.

2. Formulation and stationary response

We consider a vertical pressure source $\mathcal{P}(x, t)$ applied at the interface of a deep, inviscid, irrotational fluid of density ρ, surface tension γ and gravity g, and translating along it at constant speed V. The unperturbed interface lies on the $z = 0$ plane, and the source moves along the x-axis, its centre at $x = -Vt$ (with $V \ge 0$). Its amplitude is modulated harmonically at frequency Ω,

https://doi.org/10.1017/jfm.2026.12145 Published online by Cambridge University Press

$$\mathcal{P}(x,t) = p_e(x+Vt)\ \cos(\Omega t), \tag{2.1}$$

where $p_e(x)$ is the spatial profile of the pressure distribution. The source is invariant along the transverse y-direction, so the wave field lies in the (x,z) plane and has straight crests: the surface elevation is $\zeta(x,t)$, and the wavevector has the single component k. Expanding the x-dependence in Fourier modes $\zeta(x,t) = \int_{-\infty}^{\infty} (\mathrm{d}k/2\pi)\, \mathrm{e}^{\mathrm{i}kx}\, \hat{\zeta}(k,t)$, the wavenumber k ranges over all real values; a free wave of wavenumber k oscillates at the frequency $\omega(k) = \sqrt{g|k| + (\gamma/\rho)|k|^3}$ (which depends only on $|k|$) (Lighthill 1978). Since ζ is real, $\hat{\zeta}(-k,t) = \hat{\zeta}^*(k,t)$, and it suffices to take $k>0$, for which $\omega(k) = \sqrt{gk(1+k^2/k_c^2)}$ is the capillary–gravity dispersion relation, where $k_c = \sqrt{\rho g/\gamma}$. The phase speed $c(k) \equiv \omega(k)/k$ is minimal at the capillary wavenumber k_c, where it equals c_{min}, and $\omega_c = c_{min}k_c = \sqrt{2gk_c}$; the group velocity is $c_g(k) \equiv \mathrm{d}\omega/\mathrm{d}k$. We write $\tilde{k} = k/k_c$, $\tilde{V} = V/c_{min}$ and $\tilde{\Omega} = \Omega/\omega_c$; the dispersion relation then reads $\omega(\tilde{k})/\omega_c = \sqrt{(\tilde{k}+\tilde{k}^3)/2}$, and the phase speed $c/c_{min} = \sqrt{(1+\tilde{k}^2)/(2\tilde{k})}$ is minimal at $\tilde{k}=1$. The forcing of each surface mode is set by the spatial Fourier transform of the pressure distribution p_e, $\hat{p}_e(k) = \int_{-\infty}^{\infty} p_e(x)\, \mathrm{e}^{-\mathrm{i}kx}\, \mathrm{d}x$. For definiteness we take this distribution concentrated along a line, $p_e(x) = p\,\delta(x)$. Its Fourier transform is then constant, $\hat{p}_e(k) = p$.

Linearising the equation of motion and the boundary condition at the free surface, and eliminating the velocity potential (Lighthill 1978), $\zeta(x,t)$ obeys, in Fourier space, the forced-oscillator equation

$$\partial_{tt}\hat{\zeta}(k,t) + \omega^2(k)\,\hat{\zeta}(k,t) = -\frac{k\,p}{2\rho}\left(\mathrm{e}^{\mathrm{i}\omega_{f1}t} + \mathrm{e}^{\mathrm{i}\omega_{f2}t}\right), \tag{2.2}$$

where the cosine modulation has split the forcing into two sidebands of the Doppler frequency kV,

$$\omega_{f1} = kV + \Omega, \qquad \omega_{f2} = kV - \Omega. \tag{2.3}$$

Note that, for a general pressure profile $p_e(x)$ of finite extent, the constant amplitude p on the right-hand side of (2.2) is replaced by the Fourier transform $\hat{p}_e(k)$.

The long-time solution of (2.2) is, for $k>0$,

$$\hat{\zeta}(k,t) = \frac{k\,p}{2\rho}\left[\frac{\mathrm{e}^{\mathrm{i}\omega_{f1}t}}{D_1 - 2\mathrm{i}\omega_{f1}\varepsilon} + \frac{\mathrm{e}^{\mathrm{i}\omega_{f2}t}}{D_2 - 2\mathrm{i}\omega_{f2}\varepsilon}\right], \qquad D_j = \omega_{fj}^2 - \omega^2, \tag{2.4}$$

where the Sommerfeld radiation condition is enforced by adding an infinitesimal friction, $2\varepsilon\,\partial_t\hat{\zeta}$, to the left-hand side of (2.2) (Lighthill 1978). Each radiating mode ($k>0$) appears as $\mathrm{e}^{\mathrm{i}(kx+\omega_{fj}t)}$, a wave whose crests travel at the phase velocity $-\omega_{fj}/k$. As the source advances in the $-x$ direction ($x=-Vt$), the sign of ω_f sets which way these crests travel: $\omega_f>0$ moves them in the same direction as the source ($-x$; prograde), $\omega_f<0$ in the opposite direction ($+x$; retrograde).

The radiating modes are the real positive roots of D_j; in dimensionless form $D_j \propto -P_j(\tilde{k})$, introducing the two cubic polynomials that organise the whole analysis

$$P_1(\tilde{k}) = \tilde{k}^3 - 2\tilde{V}^2\tilde{k}^2 + (1-4\tilde{V}\tilde{\Omega})\,\tilde{k} - 2\tilde{\Omega}^2, \tag{2.5}$$

$$P_2(\tilde{k}) = \tilde{k}^3 - 2\tilde{V}^2\tilde{k}^2 + (1+4\tilde{V}\tilde{\Omega})\,\tilde{k} - 2\tilde{\Omega}^2. \tag{2.6}$$

Three of their roots recur below: $\tilde{k}_u$ and $\tilde{k}_*$, the smallest positive root of P_1 and the retrograde root of P_2 (both long-wavelength modes, $\sim\tilde{\Omega}^2$, at small $\tilde{\Omega}$), and $\tilde{k}_d$, a double

https://doi.org/10.1017/jfm.2026.12145 Published online by Cambridge University Press

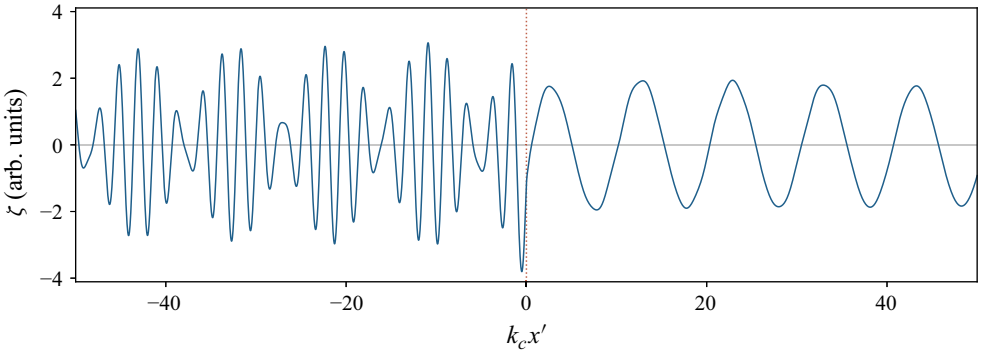


Figure 1. Interface profile $\zeta(x')$ in the source frame ($x' = x + Vt$) at $t/T = 0$, $T = 2\pi/\Omega$, from (2.4), for $\tilde{V} = 1.3$, $\tilde{\Omega} = 0.15$: two short capillary ripples ($\tilde{k} \approx 2.7$ and 3.3) on one side; a longer wave ($\tilde{k} \approx 0.62$) with a slowly varying long-wave mode ($\tilde{k} \approx 0.03$) on the other. The source is located at $x' = 0$ (dotted line).

root, one at each radiation transition. The damping term in (2.4), $-2\mathrm{i}\omega_{fj}\varepsilon$, makes the radiation condition enter with the sign of ω_{fj}: negative for the upper sideband, reversed for the lower one once $\Omega > kV$. The interface profile was first studied by Pramanik (1980); a representative one is shown in figure 1. How many of these roots are real and positive – and hence which waves radiate – depends on $(\tilde{V}, \tilde{\Omega})$; the resulting partition of the plane into four radiation regimes is the phase diagram of figure 2 (§ 4).

3. Mean wave resistance

The wave resistance is the streamwise force exerted by the fluid on the source (Havelock 1918), reckoned positive when it opposes the motion

$$R(t) = -\int_{-\infty}^{+\infty} \mathcal{P}(x,t)\,\partial_x \zeta(x,t)\,\mathrm{d}x, \tag{3.1}$$

where $\mathcal{P}(x,t)$ is given by (2.1). Using Parseval's theorem, we substitute (2.4) and average over a modulation period; only the $\cos^2 \Omega t$ contributions survive, giving

$$\langle R\rangle = \int_0^\infty \frac{k^2 p^2}{\rho}\left[\frac{\omega_{f1}\varepsilon}{D_1^2 + 4\omega_{f1}^2\varepsilon^2} + \frac{\omega_{f2}\varepsilon}{D_2^2 + 4\omega_{f2}^2\varepsilon^2}\right]\frac{\mathrm{d}k}{2\pi}. \tag{3.2}$$

In the radiation limit $\varepsilon \to 0^+$ each Lorentzian collapses onto a signed delta, $\omega_f\varepsilon/(D^2 + 4\omega_f^2\varepsilon^2) \to (\pi/2)\,\mathrm{sgn}(\omega_f)\,\delta(D)$, and the integral reduces to a sum of residues over the roots of P_1 and P_2. In terms of the dimensionless wavenumber $\tilde{k} = k/k_c$, this gives

$$\langle \tilde{R}\rangle \equiv \frac{\langle R\rangle}{p^2/\gamma} = \frac{1}{4}\big(\tilde{S}_1 + \tilde{S}_2^{>} - \tilde{S}_2^{<}\big), \tag{3.3}$$

where

$$\tilde{S}_1 = \sum_{\substack{P_1(\tilde{k}_n)=0 \\ \tilde{k}_n>0}} \frac{\tilde{k}_n^2}{|P_1'(\tilde{k}_n)|}, \qquad \tilde{S}_2^{\gtrless} = \sum_{\substack{P_2(\tilde{k}_n)=0 \\ \tilde{k}_n\tilde{V}\gtrless\tilde{\Omega}}} \frac{\tilde{k}_n^2}{|P_2'(\tilde{k}_n)|}. \tag{3.4}$$

https://doi.org/10.1017/jfm.2026.12145 Published online by Cambridge University Press

The three sums in (3.4) are non-negative and enter (3.3) with the sign of ω_{ff}: since $\omega_{f1} = kV + \Omega > 0$ at every $k > 0$, $\tilde{S}_1$ enters with a plus, as do the prograde lower-sideband waves, the retrograde ones with a minus. Writing $\tilde{\omega}(\tilde{k}) = \omega/\omega_c$, one has $P_j = 2[\tilde{\omega}^2 - (\tilde{k}\tilde{V} \pm \tilde{\Omega})^2]$, so the positive roots of P_1 solve $\tilde{\omega} - \tilde{k}\tilde{V} = \tilde{\Omega}$, and those of P_2 solve $\tilde{\omega} - \tilde{k}\tilde{V} = -\tilde{\Omega}$ (prograde) or $\tilde{\omega} + \tilde{k}\tilde{V} = \tilde{\Omega}$ (retrograde). The last equation has exactly one root $\tilde{k}_*$, its left-hand side rising monotonically from 0 to ∞: there is always exactly one retrograde wave.

The three sums combine in (3.3) with $\tilde{S}_2^<$ subtracted, so $\langle R \rangle$ is not manifestly positive. It is nevertheless strictly positive for every $\tilde{V} > 0$ and $\Omega \neq 0$. To prove this, let $\tilde{k}_u$ be the smallest positive root of P_1, which exists since $P_1(0) = -2\tilde{\Omega}^2 < 0$. Because $\tilde{\omega} + \tilde{k}\tilde{V} > \tilde{\omega} - \tilde{k}\tilde{V}$ for $\tilde{k} > 0$, the retrograde root $\tilde{k}_*$ lies below $\tilde{k}_u$; and the identity $\tilde{\omega}\, c_g/c_{min} = (1 + 3\tilde{k}^2)/4$ then gives $\tilde{k}_u^2/P_1'(\tilde{k}_u) > \tilde{k}_*^2/P_2'(\tilde{k}_*)$. (This inequality follows from the derivatives: with $\tilde{\omega}_u = \tilde{k}_u\tilde{V} + \tilde{\Omega}$ and $\tilde{\omega}_* = \tilde{\Omega} - \tilde{k}_*\tilde{V}$ the dispersion at the two roots, both positive, $P_1'(\tilde{k}_u) = 1 + 3\tilde{k}_u^2 - 4\tilde{V}\tilde{\omega}_u$ and $P_2'(\tilde{k}_*) = 1 + 3\tilde{k}_*^2 + 4\tilde{V}\tilde{\omega}_*$. The second is positive term by term; the first is non-negative, $\tilde{k}_u$ being the first root of P_1, and vanishes only at a radiation transition, where $\langle R \rangle$ diverges. Except at a transition, both denominators are positive, and the inequality is equivalent to $\tilde{k}_u^2 P_2'(\tilde{k}_*) - \tilde{k}_*^2 P_1'(\tilde{k}_u) > 0$. In this difference the $3\tilde{k}_u^2\tilde{k}_*^2$ terms cancel, leaving $\tilde{k}_u^2 - \tilde{k}_*^2 + 4\tilde{V}(\tilde{k}_u^2\tilde{\omega}_* + \tilde{k}_*^2\tilde{\omega}_u)$, positive since $\tilde{k}_* < \tilde{k}_u$.) The left-hand side is one term of $\tilde{S}_1$ and the right-hand side is all of $\tilde{S}_2^<$, so $\tilde{S}_1 > \tilde{S}_2^<$: the single upper-sideband wave $\tilde{k}_u$ already outweighs the retrograde one $\tilde{k}_*$, which therefore cannot reverse the balance. We conclude that the mean wave resistance $\langle R \rangle$ is always positive, and vanishes only on the steady below-threshold axis $\Omega = 0$, $\tilde{V} < 1$, where nothing is radiated, and on the axis $\tilde{V} = 0$, where a source that does not advance radiates symmetrically. Note that the sign of the instantaneous wave resistance $R(t) = \langle R \rangle(1 + \cos 2\Omega t) - C \sin 2\Omega t$ (with C the reactive, non-radiating amplitude) varies in time, dipping to $\langle R \rangle - \sqrt{\langle R \rangle^2 + C^2} < 0$ within each period.

The identity used above also recasts (3.3) in far-field form: it gives $|P_j'(\tilde{k}_n)| = 4\tilde{\omega}_n|\tilde{c}_{g,n} - \epsilon_n\tilde{V}|$ with $\epsilon_n = \mathrm{sgn}(\omega_{f,n})$ and $\tilde{c}_{g,n} = c_g(\tilde{k}_n)/c_{min}$, so that each term is an energy flux and $\langle R \rangle = \sum_n (k_n/\omega_{f,n})\Phi_n$, with Φ_n the power radiated by mode n (Grue & Palm 1985). This does not supersede the residue calculation. A pulsating source works through its oscillation as well as its advance, so the energy budget reads $\Phi_{tot} = V\langle R \rangle + \Omega W$, with W the pulsation contribution: conservation fixes this sum but not $\langle R \rangle$ separately, and only the residues disentangle them.

4. Below-threshold radiation and the phase diagram

The central consequence of (3.3) is immediate. For any $\Omega \neq 0$ the small root $\tilde{k}_*$ of P_2 exists at any speed $V > 0$: a genuinely propagating mode, radiating power to infinity. It is retrograde ($\omega_{f2} < 0$) and thus enters the residue sum (3.3) through the subtracted term $\tilde{S}_2^<$. The upper sideband is never silent either: $P_1(0) = -2\tilde{\Omega}^2 < 0$ guarantees a positive root $\tilde{k}_u$ of P_1 for every $\Omega \neq 0$, and by the inequality of § 3 that single wave already outweighs the retrograde one $\tilde{k}_*$, so that $\langle R \rangle > 0$. The steady threshold $V = c_{min}$ therefore does not carry over to the modulated problem – as soon as the source oscillates, radiation occurs at all speeds, and the below-threshold silent regime of the steady source disappears.

https://doi.org/10.1017/jfm.2026.12145 Published online by Cambridge University Press

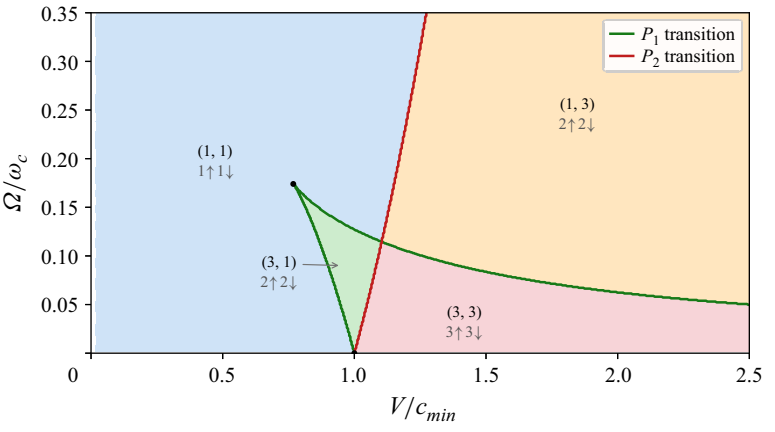


Figure 2. Phase diagram in the $(\tilde{V}, \tilde{\Omega})$ plane. Each region is labelled by the numbers (n_1, n_2) of real positive roots of (P_1, P_2) and, beneath, by the split of the radiating modes into upstream (↑, energy ahead of the source) and downstream (↓, behind); the two counts are equal in every region (the narrow (3, 1) region is labelled via an arrow). The green and red curves are the radiation transitions of P_1 and P_2; both emanate from the bifurcation point $(\tilde{V}, \tilde{\Omega}) = (1, 0)$, and the cusp of the P_1 curve lies at $(\tilde{V}, \tilde{\Omega}) \approx (0.768, 0.174)$. The expression for $\langle R \rangle$ in each region is given by (3.3).

Whirligig beetles radiate below c_{min} through their leg strokes (Voise & Casas 2010), an effect ascribed to their unsteadiness (Closa *et al.* 2010); their periodicity alone suffices.

The number of radiating modes changes across radiation transitions, at which two roots of P_j coalesce into a double root $\tilde{k}_d$. This is the condition $c_g(\tilde{k}_d) = V$ on the group velocity (i.e. $c_g/c_{min} = \tilde{V}$), which traces one curve for each polynomial in the $(\tilde{V}, \tilde{\Omega})$ plane and partitions it into the four regions of the phase diagram, figure 2. The criterion, and the partition it induces – including the cusp below – were obtained by Pramanik (1980), within the general framework of Lighthill (1967). In the variables $(n\tau, \tilde{V})$ with $\tau = \Omega V/g = 2\tilde{\Omega}\tilde{V}$, where n is the harmonic index, the same partition is the phase diagram of Roccuzzo & Herault (2026, figure 13*a*), reached there independently; each point of that diagram refers to a single sideband, whereas figure 2 records the joint state (n_1, n_2) of both. Their critical point is the cusp located below, whose coordinates we give in closed form. Both transition curves emanate from the steady bifurcation point $(\tilde{V}, \tilde{\Omega}) = (1, 0)$; the P_1 curve possesses a cusp at $\tilde{k}_f = \sqrt{(2\sqrt{3} - 3)/3} \approx 0.393$, with coordinates $\tilde{V}_f = (3 - \sqrt{3})/[2(2\sqrt{3} - 3)^{1/4}] \approx 0.768$ and $\tilde{\Omega}_f = (2\sqrt{3} - 3)^{1/4}(3 - \sqrt{3})/6 \approx 0.174$.

The same criterion fixes where each radiated wave is found relative to the source: a mode sits upstream (ahead) when its energy outruns the source, downstream (behind) otherwise. A prograde mode ($\omega_{fj} > 0$) carries its energy forwards, so it sits upstream when $c_g > V$, i.e. when $P_j'(\tilde{k}_n) > 0$. A retrograde mode ($\omega_{f2} < 0$) carries its energy backwards and is therefore always downstream, as in the steady picture. Each sideband favours one side. The upper sideband (ω_{f1}) supplies one net extra upstream mode, its long prograde wave $\tilde{k}_u \sim \tilde{\Omega}^2$ at small $\tilde{\Omega}$. The lower sideband (ω_{f2}) supplies one net extra downstream mode, the retrograde long wave $\tilde{k}_*$. The radiating modes therefore split into equal numbers upstream and downstream in every region, as annotated in figure 2. This balance has no counterpart in the pure-gravity problem, where one wave travels upstream and three downstream below the resonance $\Omega V/g = 1/4$, only two downstream waves remaining

https://doi.org/10.1017/jfm.2026.12145 Published online by Cambridge University Press

above it (Kaplan 1957; Debnath & Rosenblat 1969; Dagan & Miloh 1982); the capillary–gravity case of a submerged source is treated by Debnath & Vann (1974). Surface tension adds two capillary waves, both upstream (Pramanik 1980).

The transitions leave a clear signature in $\langle R\rangle$: at a double root $P_j'(\tilde{k}_d)=0$, the term $\tilde{k}_d^2/|P_j'(\tilde{k}_d)|$ diverges and $\langle R\rangle$ develops an integrable singularity.

Close to a transition, reached at $\tilde{\Omega}=\tilde{\Omega}_d$ for a given $\tilde{V}$, the two coalescing roots form a saddle node, $\tilde{k}_\pm=\tilde{k}_d\pm\sqrt{\alpha\,(\tilde{\Omega}-\tilde{\Omega}_d)}$, with the saddle-node coefficient $\alpha=-2\,\partial_{\tilde{\Omega}}P_j/P_j''$ evaluated at $(\tilde{k}_d,\tilde{\Omega}_d)$, so that $|P_j'(\tilde{k}_\pm)|\propto|\tilde{\Omega}-\tilde{\Omega}_d|^{1/2}$ and the resistance diverges as an integrable, one-sided square root, $\langle\tilde{R}\rangle\simeq A(\tilde{V})\,|\tilde{\Omega}-\tilde{\Omega}_d|^{-1/2}$ on the side where the pair is real (for instance $A\approx0.11$ at $\tilde{V}=0.95$). This square-root law degenerates at the bifurcation point $(\tilde{V},\tilde{\Omega})=(1,0)$, where the coalescence is pinned at the dispersion minimum $\tilde{k}=1$ and the two transition curves originate. There the steady limit of $\langle\tilde{R}\rangle$ already diverges as $\langle\tilde{R}\rangle\simeq(1/4)(\tilde{V}-1)^{-1/2}$ along $\tilde{\Omega}=0$, while along the threshold $\tilde{V}=1$ the modulated wave resistance diverges as $\langle\tilde{R}\rangle\simeq(1/8)\,\tilde{\Omega}^{-1/2}$ as $\tilde{\Omega}\to0$; the bifurcation point is thus the common origin of the steady and modulated square-root singularities. At the cusp of the P_1 curve the two saddle-node branches meet, the radiating root becoming triple, and the one-sided square root is replaced by a stronger, two-sided divergence $\langle\tilde{R}\rangle\propto|\tilde{\Omega}-\tilde{\Omega}_\mathrm{f}|^{-2/3}$ (figure 3*b*). Conversely, for $\tilde{V}$ below the cusp speed a vertical cut meets no P_1 transition and $\langle R\rangle$ rises smoothly as $\tilde{\Omega}^5$ at small $\tilde{\Omega}$ to a broad maximum without resonance, after which it decays as $\tilde{\Omega}^{-1/3}$ (figure 3*a*).

Just below the steady threshold, by contrast, a vertical cut does cross both P_1 transitions and $\langle R\rangle$ exhibits sharp resonant peaks (figure 3*c*): a slow modulation of a marginally below-threshold source suffices to trigger a pronounced radiative response.

5. Limiting and asymptotic behaviour

As $\Omega\to0^+$ the two long sideband roots $\tilde{k}_u$ and $\tilde{k}_*$ tend to zero and their contributions vanish, while the remaining roots of P_1 and P_2 merge onto those of $P_0(\tilde{k})=\tilde{k}^3-2\tilde{V}^2\tilde{k}^2+\tilde{k}$. The formula (3.3) then reduces to $\langle\tilde{R}\rangle=(1/2)\sum_{P_0(\tilde{k}_n)=0,\,\tilde{k}_n>0}\tilde{k}_n^2/|P_0'(\tilde{k}_n)|$, which is zero for $\tilde{V}<1$ (no real positive root of P_0) and positive for $\tilde{V}>1$. This is exactly one half of the steady RdG resistance (1.1), the factor $(1/2)$ being the time-average $\langle\cos^2\Omega t\rangle$ of the modulation.

In the drag-free corner of the steady problem ($V<c_{min}$, small Ω), the long roots $\tilde{k}_u$ and $\tilde{k}_*$ are nearly degenerate and their residues almost cancel, leaving

$$\langle\tilde{R}\rangle\xrightarrow[\tilde{\Omega}\to0]{}24\,\tilde{V}\,\tilde{\Omega}^5. \tag{5.1}$$

At the opposite end the radiating wavenumbers grow without bound, $\tilde{k}_n\sim\tilde{\Omega}^{2/3}$; at such large $\tilde{k}$ the capillary term $\tilde{k}^3$ dominates the dispersion relation over the gravity term $\tilde{k}$, so the radiated waves are short, pure-capillary ripples. The order-$\tilde{\Omega}^0$ terms cancel, and

$$\langle\tilde{R}\rangle\xrightarrow[\tilde{\Omega}\to\infty]{}\frac{2^{1/3}}{9}\,\tilde{V}\,\tilde{\Omega}^{-1/3}, \tag{5.2}$$

with the universal coefficient $2^{1/3}/9\approx0.140$. Since c_{min} enters only through the scales, below- and above-threshold sources alike approach the same capillary decay, differing only through the prefactor $\propto\tilde{V}$. Below threshold this raises $\langle R\rangle$ from zero; above threshold

https://doi.org/10.1017/jfm.2026.12145 Published online by Cambridge University Press

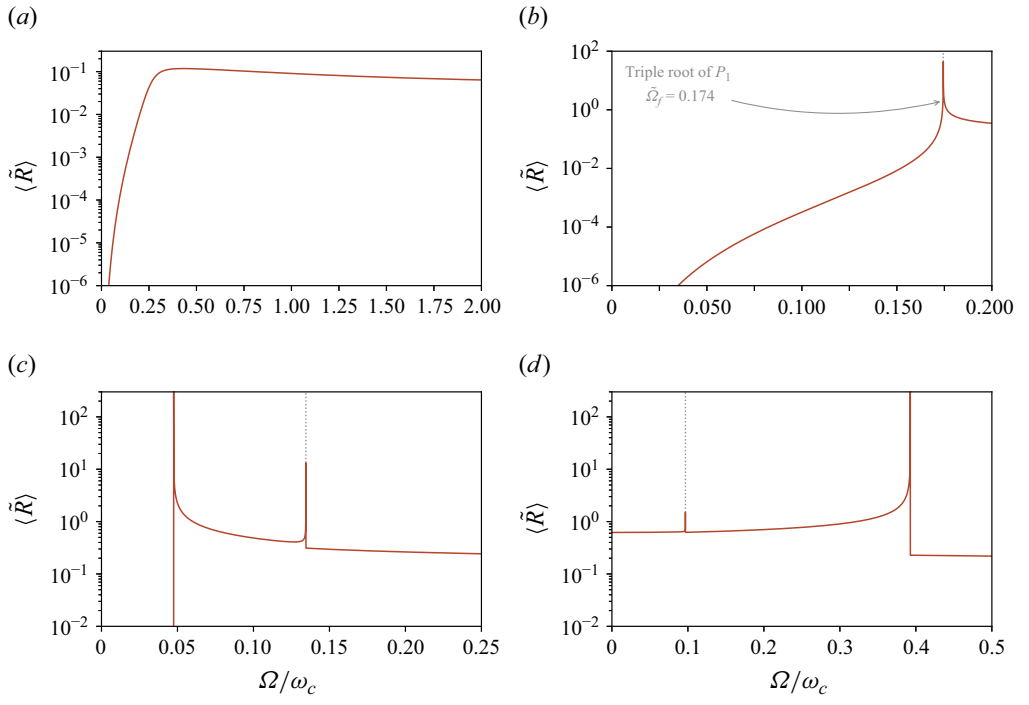


Figure 3. Dimensionless mean wave resistance $\langle\tilde{R}\rangle = \langle R\rangle/(p^2/\gamma)$ (logarithmic scale) versus $\tilde{\Omega} = \Omega/\omega_c$ at four fixed speeds, sweeping V through the P_1 cusp and the steady threshold. Throughout, $\langle\tilde{R}\rangle$ diverges integrably at the radiation transitions (dotted asymptotes), where a radiating root of P_1 or P_2 becomes double, and stays finite elsewhere; it decays as $\tilde{\Omega}^{-1/3}$ at high frequency. (*a*) At $V = 0.5\,c_{min}$, below the cusp speed, the vertical cut meets no P_1 transition: $\langle\tilde{R}\rangle$ rises as $\tilde{\Omega}^5$ at small $\tilde{\Omega}$ and passes a broad maximum, without any resonance. (*b*) At the cusp speed $V = 0.768\,c_{min}$ the two P_1 saddle-node branches meet and the radiating root becomes triple at $\tilde{\Omega}_f = 0.174$, where $\langle\tilde{R}\rangle$ diverges on both sides as $|\tilde{\Omega} - \tilde{\Omega}_f|^{-2/3}$. (*c*) At $V = 0.95\,c_{min}$, although $V < c_{min}$, the source radiates at every $\Omega \neq 0$ ($\langle\tilde{R}\rangle$ vanishes only at $\Omega = 0$ and is too small to be visible before the first transition), crossing two P_1 transitions ($\tilde{\Omega} \approx 0.048,\ 0.134$). (*d*) Above threshold, $V = 1.3\,c_{min}$, the resistance starts from its finite steady value, crosses a low-amplitude P_1 resonance ($\tilde{\Omega} \approx 0.097$) and a high-amplitude P_2 resonance ($\tilde{\Omega} \approx 0.393$) – both integrable divergences, of very different prefactor – beyond which a radiating mode disappears and the resistance drops.

it drives $\langle R\rangle$ well below the steady RdG value. Finally, for $V \to \infty$ at fixed Ω the radiation is carried by short capillary ripples ($\tilde{k}_n \sim 2\tilde{V}^2$) and the resistance flattens onto a plateau, $\langle\tilde{R}\rangle \to (1/2) + \tilde{\Omega}/(4\tilde{V}^3) + 3/(16\tilde{V}^4)$. The leading $(1/2)$ is again $\langle\cos^2\Omega t\rangle$, but that factor fails at higher order – the $\tilde{V}^{-4}$ coefficient is $3/16$, not the $1/4$ that a uniform halving of the steady result (1.1) would give – so the expansion is non-analytic at $\Omega = 0$ and the limits $V \to \infty$ and $\Omega \to 0$ do not commute.

Because each radiating mode contributes to $\langle R\rangle$ in proportion to $\tilde{k}_n^2$ (3.4), the resistance is dominated by the short, capillary-scale waves throughout most of the $(\tilde{V}, \tilde{\Omega})$ plane – everywhere, that is, except the below-threshold corner where the radiated waves are long. As a result the two single-physics reductions – approximating the dispersion relation by capillarity alone or by gravity alone – are far from equally accurate. In both we retain the full physical system, so that c_{min} and ω_c remain well defined, and simplify only the dispersion relation used to compute the radiated field. Retaining only the capillary term ($\omega^2 = \gamma k^3/\rho$) reproduces $\langle R\rangle$ to within a few per cent wherever the radiating waves are

https://doi.org/10.1017/jfm.2026.12145 Published online by Cambridge University Press

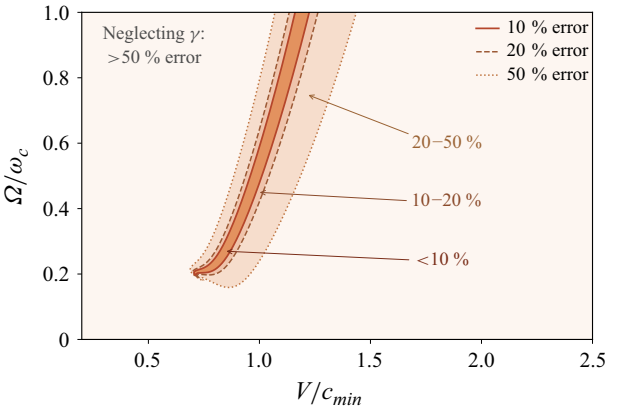


Figure 4. Failure of the pure-gravity approximation for the mean wave resistance $\langle R\rangle$ of a line source, obtained by discarding surface tension (dispersion $\omega^2 = gk$). Contours mark the relative error reaching 10 % (solid), 20 % (dashed) and 50 % (dotted): the approximation is accurate to within 10 % only along the thin band where its single gravity branch happens to mimic the exact response, while the error exceeds 50 % over most of the $(\tilde{V}, \tilde{\Omega})$ plane. Neglecting γ thus misrepresents $\langle R\rangle$ almost everywhere.

short, at high speed ($\tilde{V} \gtrsim 2$) or high frequency; but it has no threshold, and below c_{min} at small $\tilde{\Omega}$ it misses the near cancellation of residues, so that by the analysis of (5.1) it overestimates $\langle R\rangle$ by orders of magnitude. Discarding surface tension instead, that is using the pure-gravity dispersion $\omega^2 = gk$, misrepresents $\langle R\rangle$ by more than 10 % over almost the entire $(\tilde{V}, \tilde{\Omega})$ plane (figure 4): although γ is dynamically negligible for the long gravity waves, it controls the short, dominant capillary-scale waves and therefore $\langle R\rangle$ itself almost everywhere.

For a source of finite width b, p is replaced by $\hat{p}_e(k)$, as noted after (2.3), reweighting each radiating mode by $|\hat{p}_e(k_n)/p|^2$. The phase diagram, the divergence exponents and the $\tilde{\Omega}^5$ law are unchanged; the $\tilde{\Omega}^{-1/3}$ tail, carried by the shortest ripples, is cut off once $k_n\, b \gtrsim 1$.

6. Conclusion

We have shown that temporal modulation qualitatively changes the wave resistance of a source moving along a capillary–gravity interface. The smallest roots $\tilde{k}_u$ of P_1 and $\tilde{k}_*$ of P_2 guarantee propagating modes – and, by the inequality of § 3, a strictly positive mean wave resistance – at every speed $V > 0$ once $\Omega \neq 0$. The steady threshold $V = c_{min}$ does not survive modulation, and $\langle R\rangle$ develops integrable resonant peaks where the radiation transitions are crossed. Physically, that below-threshold radiation takes the form of very long-wavelength modes, $\tilde{k}_u \sim \tilde{k}_* \sim \tilde{\Omega}^2$ as $\tilde{\Omega} \to 0$, superposed on the localised deformation of the interface near the source.

The modulation also modifies the net displaced area. For a steady source ($\Omega = 0$) this area is finite, $\int_{-\infty}^{\infty} \zeta \, \mathrm{d}x = -p/(\rho g)$ (Lamb 1932; Raphael & de Gennes 1996). Under modulation ($\Omega \neq 0$), the displaced area vanishes at every instant, as follows from (2.4) in the limit $k \to 0$: $\int_{-\infty}^{\infty} \zeta \, \mathrm{d}x = \hat{\zeta}(0, t) = 0$ for every V. The displaced area thus jumps discontinuously at $\Omega = 0$, from $-p/(\rho g)$ to zero.

In each opposite single-scale limit the response reduces to one critical resonance: without surface tension we recover, within linear theory, the resonance $\Omega V/g = 1/4$ of the

https://doi.org/10.1017/jfm.2026.12145 Published online by Cambridge University Press

classical translating–pulsating gravity-wave source (Kaplan 1957; Dagan & Miloh 1982); in the gravity-free limit ($g \to 0$) the theory predicts its capillary counterpart, a single critical condition $\Omega\gamma/(\rho V^3) = 4/27$, with resonant wavenumber $k_d = 4\rho V^2/(9\gamma)$, the capillary scaling $\Omega \propto V^3$ contrasting with the $\Omega \propto V^{-1}$ scaling of the gravity resonance.

The results apply to interfacial objects whose forcing is periodically modulated as they translate. Two extensions follow. The first, whose leading effect is given in § 5, replaces the line source by one of finite width. For the second, a point disturbance free to radiate over the whole free surface, the Doppler shift becomes $kV\cos\theta$; P_1 and P_2 are then recovered at each angle with $\tilde{V} \to \tilde{V}\cos\theta$, so that the positivity of § 3 survives *a fortiori*, and angular integration turns the resonant divergences into finite jumps, the steady limit being the discontinuity of Raphael & de Gennes (1996, equation (2.36)) at $V = c_{min}$. The analysis is linearised throughout and the fluid inviscid: the nonlinear capillary–gravity problem (Dias & Kharif 1999) remains open, and since viscosity keeps the steady resistance bounded as $V \to c_{min}$ (Richard & Raphael 1999), how it tempers the resonant divergences is a natural further direction. Experimentally, such a forcing could be realised by a vertically oscillating microprobe or atomic force microscope tip in tapping mode, whose lateral force measures $\langle R \rangle$ directly, or contactlessly by an amplitude-modulated acoustic radiation pressure.

Acknowledgements. H.D. is grateful to the Gulliver laboratory, ESPCI Paris, for its hospitality.

Funding. H.D. acknowledges support from the Israel Science Foundation (Grant No. 1611/24).

Declaration of interests. The authors report no conflicts of interest.

Data availability statement. The scripts supporting this study are available from the corresponding authors on reasonable request.

References

Arutkin, M., Reuveni, S. & Raphael, E. 2026 Wave resistance for stochastic motion at interfaces. arXiv:2606.08732.

Chepelianskii, A.D., Chevy, F. & Raphael, E. 2008 Capillary-gravity waves generated by a slow moving object. *Phys. Rev. Lett.* **100**, 074504.

Closa, F., Chepelianskii, A.D. & Raphael, E. 2010 Capillary-gravity waves generated by a sudden object motion. *Phys. Fluids* **22**, 052107.

Dagan, G. & Miloh, T. 1982 Free-surface flow past oscillating singularities at resonant frequency. *J. Fluid Mech.* **120**, 139–154.

Debnath, L. & Rosenblat, S. 1969 The ultimate approach to the steady state in the generation of waves on a running stream. *Q. J. Mech. Appl. Maths* **22**, 221–233.

Debnath, L. & Vann, J.M. 1974 Propagation of water waves with surface tension due to submerged sources. *Bull. Acad. Polon. Sci. Sér. Sci. Techn.* **22**, 539–546.

Dias, F. & Kharif, C. 1999 Nonlinear gravity and capillary-gravity waves. *Annu. Rev. Fluid Mech.* **31**, 301–346.

Dode, A., Carmigniani, R., Cohen, C., Clanet, C. & Bocquet, L. 2022 Wave drag during an unsteady motion. *J. Fluid Mech.* **951**, A15.

Froude, W. 1874 Experiments with H.M.S. Greyhound. *Trans. Inst. Nav. Archit.* **15**, 36–73.

Grue, J. & Palm, E. 1985 Wave radiation and wave diffraction from a submerged body in a uniform current. *J. Fluid Mech.* **151**, 257–278.

Havelock, T.H. 1918 Wave resistance: some cases of three-dimensional fluid motion. *Proc. R. Soc. Lond. A* **95**, 354–365.

Kaplan, P. 1957 The waves generated by the forward motion of oscillatory pressure distributions. In *Proceedings of the Fifth Midwestern Conference on Fluid Mechanics*, pp. 316–329.

Kelvin, Lord 1887 On ship waves. *Proc. Inst. Mech. Engrs* **38**, 409–434.

Lamb, H. 1932 *Hydrodynamics*, 6th edn. Cambridge University Press (Reprinted 1993).

Lighthill, M.J. 1967 On waves generated in dispersive systems by travelling forcing effects, with applications to the dynamics of rotating fluids. *J. Fluid Mech.* **27**, 725–752.

https://doi.org/10.1017/jfm.2026.12145 Published online by Cambridge University Press

LIGHTHILL, M.J. 1978 *Waves in Fluids*. Cambridge University Press.

PRAMANIK, A.K. 1980 Capillary-gravity waves produced by a moving pressure distribution. *Z. Angew. Math. Phys.* **31**, 174–180.

RAPHAEL, E. & DE GENNES, P.-G. 1996 Capillary gravity waves caused by a moving disturbance: wave resistance. *Phys. Rev. E* **53**, 3448–3455.

RICHARD, D. & RAPHAEL, E. 1999 Capillary-gravity waves: the effect of viscosity on the wave resistance. *Europhys. Lett.* **48**, 49–52.

ROCCUZZO, M. & HERAULT, J. 2026 Transitions in unsteady capillary-gravity wakes of surface swimmers. *Phys. Rev. Fluids* **11**, 044805.

VOISE, J. & CASAS, J. 2010 The management of fluid and wave resistances by whirligig beetles. *J. R. Soc. Interface* **7**, 343–352.

https://doi.org/10.1017/jfm.2026.12145 Published online by Cambridge University Press